Current Biology 21, 2033–2045, December 20, 2011 ©2011 Elsevier Ltd All rights reserved DOI 10.1016/j.cub.2011.10.054

Article

LIN-42/PERIOD Controls Cyclical and Developmental Progression of *C. elegans* Molts

Gabriela C. Monsalve,[1] Cheryl Van Buskirk,[2] and Alison R. Frand[1,*]
[1]Department of Biological Chemistry, David Geffen School of Medicine, University of California, Los Angeles, Los Angeles, CA 90095, USA
[2]Department of Biology, California State University, Northridge, Northridge, CA 91330, USA

Summary

Background: Biological timing mechanisms that integrate cyclical and successive processes are not well understood. *C. elegans* molting cycles involve rhythmic cellular and animal behaviors linked to the periodic reconstruction of cuticles. Molts are coordinated with successive transitions in the temporal fates of epidermal blast cells, which are programmed by genes in the heterochronic regulatory network. It was known that juveniles molt at regular 8–10 hr intervals, but the anticipated pacemaker had not been characterized.
Results: We find that inactivation of the heterochronic gene *lin-42a*, which is related to the core circadian clock gene *PERIOD* (*PER*), results in arrhythmic molts and continuously abnormal epidermal stem cell dynamics. The oscillatory expression of *lin-42a* in the epidermis peaks during the molts. Further, forced expression of *lin-42a* leads to anachronistic larval molts and lethargy in adults.
Conclusions: Our results suggest that rising and falling levels of LIN-42A allow the start and completion, respectively, of larval molts. We propose that LIN-42A and affiliated factors regulate molting cycles in much the same way that PER-based oscillators drive rhythmic behaviors and metabolic processes in mature mammals. Further, the combination of reiterative and stage-specific functions of LIN-42 may coordinate periodic molts with successive development of the epidermis.

Introduction

Diverse timing mechanisms control cyclical and successive biological events. Biological clocks synchronize rhythmic behaviors and metabolic processes with predictable extrinsic and intrinsic cues. The best-characterized clocks are circadian oscillators composed of interconnected feedback loops among PERIOD (PER) proteins and other transcriptional regulators, and dysfunction of PER proteins contributes to various human sleep disorders, metabolic syndromes, and cancers [1–4]. However, the role of PER proteins and related oscillators in development has not been examined. Hormones and related gene regulatory cascades control many progressive transitions in animal development [5–7]. However, the means by which external and internal cues affect the pace of development are not well understood.

C. elegans provides a useful model to study the integration of cyclical and successive events in metazoan development. *C. elegans* molting cycles involve rhythmic cellular and animal behaviors linked to the repeated synthesis and removal of larval exoskeletons and related attachments to underlying epidermal cells and syncytia [8–11]. The nematode exoskeleton (cuticle) is a complex, multilayered extracellular matrix (ECM) composed mainly of collagens [12]. The cuticle is remade four times during sleep-like episodes of behavioral quiescence (lethargus), which are regulated by neuroendocrine signaling [13–15]. Thereafter, animals escape from the old cuticle (ecdyse) through a series of idiosyncratic movements. Juveniles molt at regular 8 to 10 hr intervals when cultivated at 25°C, but the timing mechanism has not been defined [16].

The heterochronic gene regulatory network programs the successive temporal identities of epidermal stem cells, which undergo stage-specific patterns of cell division and differentiation and also contribute to the synthesis of new cuticles during every larval stage [17, 18]. These progressive transitions in epidermal fates are coordinated with rhythmic molts, but the related molecular mechanism is not understood. Most heterochronic genes are expressed during specific developmental stages [16]. Mutations in the *lin-4* and *let-7* microRNAs (miRNAs) and other heterochronic genes affect the number of molts in the life cycle but have not been reported to affect the time between molts [19–21]. In contrast, expression of the heterochronic gene *lin-42*, which is homologous to human PER, oscillates in phase with molting cycles [22]. The significance of the temporally reiterated expression of *lin-42* was not known, because the anticipated periodic functions of *lin-42* had not been described [23, 24]. Here, we show that *lin-42a* regulates the timing and execution of rhythmic molts, as well as continuous development of the epidermis. We propose that cyclical and stage-specific actions of LIN-42/PER coordinate these essential, interdependent processes.

Results

LIN-42A Is Required for Rapid, Rhythmic, and Productive Molting Cycles

The *lin-42* locus of *C. elegans* encodes several distinct proteins related to mammalian and insect PER [23]. The LIN-42B isoform contains a PAS (Period/Ant/Sim) domain as well as Ser-Tyr-Gln (SYQ) and Leu-Thr (LT) sequence motifs conserved in human PER1 (see Figure S1A available online). LIN-42C contains the PAS domain and unique C-terminal residues; LIN-42A contains the SYQ and LT motifs and unique N-terminal residues. Previous studies identified the downstream region of the *lin-42* locus as essential for development [23], but the reference allele *lin-42(n1089)* is an upstream deletion, which does not affect the coding sequence of *lin-42a* (Figure S1B).

To evaluate the role of *lin-42* in the regulation of molting cycles, we obtained the deletion allele *lin-42(ok2385)* from the *C. elegans* Knockout Consortium. This downstream deletion encompasses the coding sequence of *lin-42a* and overlapping exons of *lin-42b* (Figure S1B). Accordingly, transcripts of *lin-42a* and *lin-42b* were not detected in extracts of *lin-42(ok2385)* mutants by RT-PCR (Figure S1C). Prior to characterizing phenotypes associated with *lin-42(ok2385)*,

*Correspondence: afrand@mednet.ucla.edu

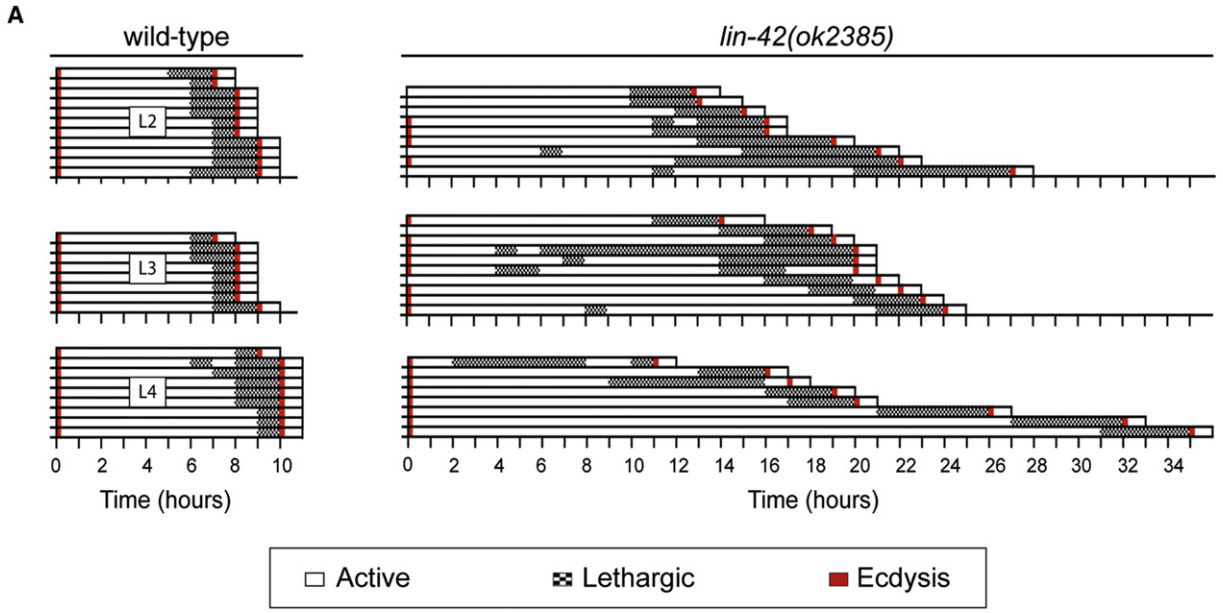

B

		Wild-type		*lin-42(ok2385)*		*Ex[lin-42a] lin-42(ok2385)*		*lin-42(n1089)*		*Ex[lin-42a] lin-42(n1089)*		*Ex[nhr-72p::lin-42a] lin-42(ok2385)*	
	Time:	hrs	Cv	hrs	Cv	hrs	Cv	hrs	Cv	hrs	Cv	hrs	Cv
L2	Active	6.6 ± 0.1	0.11	12.6 ± 0.9	0.22	7.3 ± 0.3	0.14	7.3 ± 0.3	0.12	--	--	--	--
	Lethargic	1.7 ± 0.1	0.32	5.1 ± 0.8	0.47	2.1 ± 0.2	0.29	2.6 ± 0.2	0.31	--	--	--	--
	Total	**8.3 ± 0.1**	**0.08**	**17.7 ± 1.5**	**0.25**	**9.4 ± 0.4**	**0.12**	**9.8 ± 0.2**	**0.08**	**--**	**--**	**--**	**--**
	N	29		9		9		12		--		--	
	P	--		<0.001		0.01		<0.001		--		--	
L3	Active	6.8 ± 0.2	0.09	14.9 ± 1.4	0.30	6.2 ± 0.2	0.09	7.3 ± 0.2	0.10	6.1 ± 0.1	0.08	--	--
	Lethargic	1.4 ± 0.2	0.37	4.6 ± 1.1	0.75	2.1 ± 0.1	0.25	2.5 ± 0.2	0.21	1.4 ± 0.2	0.53	--	--
	Total	**8.4 ± 0.3**	**0.13**	**19.1 ± 1.3**	**0.22**	**8.3 ± 0.2**	**0.08**	**9.8 ± 0.3**	**0.09**	**7.5 ± 0.2**	**0.10**	**--**	**--**
	N	10		10		12		12		15		--	
	P	--		<0.001		0.70		<0.01		0.04		--	
L4	Active	8.1 ± 0.2	0.09	17.4 ± 3.1	0.50	8.5 ± 0.3	0.10	10.8 ± 0.6	0.19	7.3 ± 0.2	0.13	6.7 ± 0.4	0.20
	Lethargic	1.8 ± 0.2	0.39	4.1 ± 0.4	0.27	3.4 ± 0.2	0.21	3.4 ± 0.4	0.37	3.0 ± 0.2	0.27	2.6 ± 0.2	0.21
	Total	**9.9 ± 0.1**	**0.05**	**21.8 ± 3.1**	**0.40**	**11.9 ± 0.3**	**0.08**	**14.1 ± 0.7**	**0.16**	**10.7 ± 0.4**	**0.15**	**9.1 ± 0.3**	**0.10**
	N	16		8		10		10		16		9	
	P	--		<0.01		<0.001		<0.001		0.09		0.64	

Figure 1. Prolonged and Irregular Molting Cycles of *lin-42(ok2385)* Larvae

(A) Each bar depicts the behavior and development of a single animal cultivated at 25°C. Larvae were collected late in the preceding stage and allowed to shed the preexisting cuticle. Time 0 corresponded to the resumption of feeding in the L2-, L3-, or L4-stage, as indicated. Thereafter, larvae were observed for 30 s of every hr and scored as described in the text.

(B) Summary of the developmental speed of animals of the indicated genotypes. Values indicate the mean duration ± SEM, the coefficient of variance (Cv), and the number of animals observed (n). The total duration of each stage included the time that animals were active, lethargic, and engaged in ecdysis. Values were compared to those of wild-type animals using unpaired, unequal Student's t tests. Molting-defective larvae were excluded from the diagrams and statistics presented in this figure.

we out-crossed the corresponding strain to wild-type animals to remove unlinked mutations.

The duration of each larval stage was measured and compared in *lin-42(ok2385)* mutants, *lin42(n1089)* mutants, and wild-type animals. In the first set of experiments, individual larvae were isolated late in the L1, L2, or L3 stage and allowed to shed the preexisting cuticle. Larvae were then observed by light microscopy for 30 s (s) of every hour (hr), until completion of the subsequent molt. Detectable contractions of the pharyngeal muscles or locomotion indicated the active, rather than lethargic, behavioral state. Observation of a larva emerging from the old cuticle or detection of a newly shed cuticle on the culture plate indicated ecdysis.

Wild-type animals completed the second, third, and fourth molts virtually in synchrony, whereas *lin-42(ok2385)* larvae completed the molts at irregular times (Figure 1). The mutants typically fed for longer and inconsistent periods, became lethargic later, and remained lethargic longer than wild-type larvae passing through the same stage. However, particular mutants were lethargic for much of the L3 and L4 stages. Eight

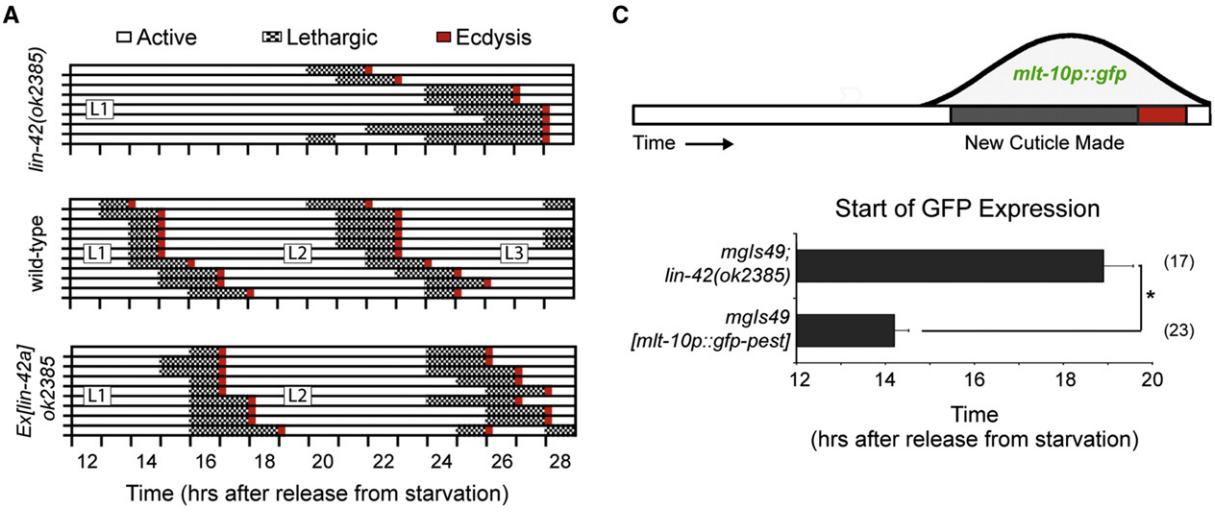

B

Genotype	Duration (hrs)					
	Active	Lethargic	Total	Cv	N	p
Wild-type	14.2 ± 0.4	1.8 ± 0.1	16.1 ± 0.4	0.13	33	--
lin-42(ok2385)	22.3 ± 0.7	3.1 ± 0.5	25.6 ± 0.9	0.10	8	<0.001
Ex[lin-42a] lin-42(ok2385)	15.0 ± 0.2	1.8 ± 0.2	16.8 ± 0.3	0.05	11	0.11
lin-42(n1089)	14.0 ± 0.3	1.8 ± 0.1	15.8 ± 0.3	0.08	20	0.51
Ex[lin-42c] lin-42(ok2385)	29.4 ± 0.9	5.7 ± 0.8	37.6 ± 0.8	0.10	19	<0.001
Ex[lin-42c]	14.5 ± 0.2	2.0 ± 0	16.5 ± 0.2	0.03	10	0.30
Ex[myo-2p::lin-42a] lin-42(ok2385)	26.6 ± 0.6	2.9 ± 0.1	29.5 ± 0.6	0.08	12	<0.001

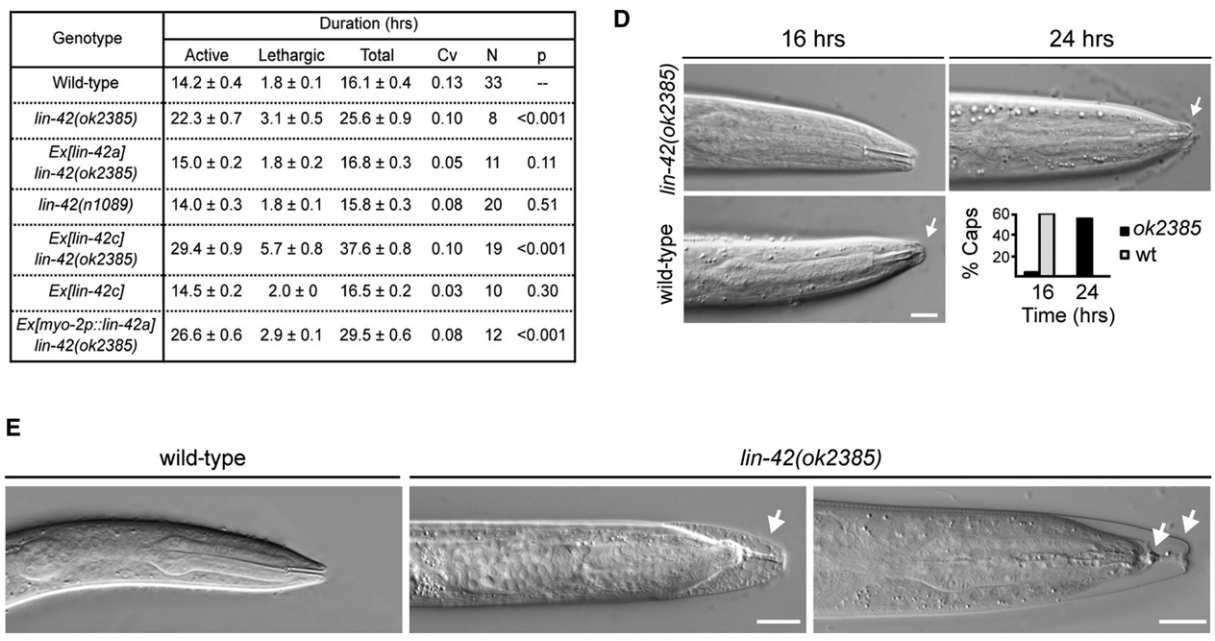

Figure 2. Delayed and Faulty Execution of the First Molt in *lin-42(ok2385)* Mutants

Early L1 animals were synchronized by starvation-induced diapause, and then fed and cultivated at 25°C.

(A) As described for Figure 1, each bar depicts the behavior and development of a single animal evaluated blind to the genotype.

(B) Summary of the duration of the L1 stage in animals of the indicated genotypes, with values and statistical analyses as described in Figure 1B. Mutants that failed to shed the L1 cuticle were excluded from these diagrams and statistics.

(C) Expression of the *mlt-10p::gfp-pest* reporter coincides with renovation of the cuticle and occurred later in *lin-42(ok2385)* mutants than control larvae. Graph shows the average time elapsed (±SEM) before detection of GFP by fluorescence microscopy. Samples sizes are indicated in parentheses. GFP was not expressed in four additional *lin-42(ok2385)* larvae observed for 20 hr. *$p < 0.001$, Student's t test.

(D) Representative differential interference contrast (DIC) images show how L1-cuticle caps (arrows) appeared on the mouths of *lin-42(ok2385)* larvae 8 hr after wild-type animals. Graph shows the prevalence of caps in the corresponding populations ($n \geq 41$).

(E) Representative images of *lin-42(ok2385)* mutants trapped either in the L1-stage cuticle (middle) or two partly shed cuticles (right) connected to the buccal capsule (arrows). Scale bars represent 10 μm.

of 27 mutants entered and exited an inactive behavioral state twice before ecdysis; four mutants exited lethargus and then took between 1 and 3 hr to ecdyse (Figure 1A). The prolonged and variable duration of larval stages became more severe as *lin-42(ok2385)* mutants developed. Strikingly, the L4 stage lasted 21.8 ± 3.1 hr (SEM) in *lin-42(ok2385)* mutants, compared with 14.1 ± 0.7 hr in *lin-42(n1089)* mutants, and 9.9 ± 0.1 hr in wild-type animals (Figure 1B). The coefficient of variance (Cv) for the total duration of the L4 stage was 0.40 for *lin-42(ok2385)* mutants, 0.16 for *lin-42(n1089)* mutants, and 0.05 for wild-type animals. Consequently, individual *lin-42(ok2385)* mutants shed the L4 cuticle up to 24 hr apart and as long as 96 hr after animals that had been synchronized by starvation-induced L1-diapause were first fed. The total duration of the L1-stage was measured using a similar approach (Figure 2A). Following release from L1-diapause,

lin-42(ok2385) mutants completed the first molt in 25.6 ± 0.9 hr (Cν = 0.10), compared with 15.8 ± 0.3 hr (Cν = 0.08) for *lin-42(n1089)* mutants, and 16.1 ± 0.4 hr (Cν = 0.13) for wild-type larvae (Figures 2A and 2B; Figure S2A).

To determine whether the irregular molting cycles of *lin-42(ok2385)* mutants were attributable to inactivation of the *lin-42a* isoform, we generated an extrachromosomal array (*aaaEx30*) containing the *lin-42a* coding sequence, fused with its endogenous promoter and 3′ untranslated region (UTR). This array restored rapid and rhythmic molting cycles in *lin-42(ok2385)* mutants (Figure 1B; Figures 2A and 2B; Figure S2B). The array also reduced the average duration of the L4 stage in *lin-42(n1089)* mutants to 10.4 ± 0.4 hr (Cν = 0.15), suggesting that the developmental delay associated with *lin-42(n1089)* resulted, in part, from decreased expression of *lin-42a* (Figure S1B). In contrast, expression of the *lin-42c* isoform from a comparable array exacerbated the delay in completion of the first molt in *lin-42(ok2385)* mutants, although the array was not toxic in wild-type animals (Figure 2B; Figure S2D). Taken together, these results indicate that *lin-42a* encodes the key factor needed to maintain rhythmic molting cycles, although *lin-42b* and *lin-42c* may also affect the pace of larval development.

We further characterized the timing of critical steps in the first molt. Synthesis of new cuticle components was indicated by expression of a transcriptional reporter for *mlt-10*, which encodes the principal member of a large family of proteins thought to act as both structural and instructive components of the cuticle [25]. Accordingly, *mlt-10* and certain cuticle collagen genes are expressed in the epidermis at nearly the same time, under control of the conserved nuclear hormone receptors (NHRs) NHR-23 and -25 [25, 26]. Expression of the *mlt-10p::gfp-pest* fusion gene was detected approximately 4.7 hr later in *lin-42(ok2385)* mutants than wild-type larvae (Figure 2C). Detachment of the preexisting cuticle from the hypoderm (apolysis) was also delayed in *lin-42(ok2385)* mutants, as indicated by the late appearance of cuticle caps over the buccal capsule (Figure 2D). Proliferation of the germline continued despite the delayed onset of the first molt (data not shown). Also, the size of particular *lin-42(ok2385)* mutants continued to increase despite prolonged retention of the L1 cuticle (Figure 2D).

Passage through L1-diapause and caloric restriction were both considered as potential explanations for the prolonged development of *lin-42(ok2385)* larvae. To test the former possibility, we transferred adults to fresh culture plates, and their offspring were allowed to develop with a constant food supply. After 20 hr of cultivation, none of 37 *lin-42(ok2385)* larvae had shed the L1 cuticle, compared with 76% (n = 45) of wild-type animals. Passage through diapause was therefore not responsible for the developmental delay. We also measured and compared the feeding rates of *lin-42(ok2385)* mutants and wild-type larvae during the mid-L4 stage, when the mutants' phenotypes were most severe. The average rate of pharyngeal contractions (pumps) in *lin-42(ok2385)* mutants was 203.4 ± 15.4 (SEM, n = 17) pumps per minute (p/m), compared with 209.3 ± 14.0 p/m (n = 13) for wild-type larvae. Malnourishment was therefore unlikely to account for the prolonged and irregular molting cycles of *lin-42(ok2385)* mutants.

A subset of *lin-42(ok2385)* mutants was unable to fully shed the preexisting cuticle at the end of the L1 and subsequent larval stages (the molting-defective, or Mlt, phenotype; Figure 2E). Such aberrant ecdyses became more common as the mutants developed; 10% (n = 10) of *lin-42(ok2385)* larvae were unable to shed the L2 cuticle, whereas 53% (n = 17) of mutants were unable to shed the L4 cuticle. Mutants that failed to ecdyse were excluded from analysis of molting cycle kinetics and related diagrams (Figure 1; Figure 2). The *aaaEx30[lin-42a]* array fully rescued the molting defects of *lin-42(ok2385)* mutants, confirming the significance of the *lin-42a* isoform for execution of the molts.

When cultivated at 20°C, 29% (n = 56) of *lin-42(ok2385)* mutants began a second molt without completing the prior ecdysis (Figure 2E, right panel). This phenomenon has not been observed in molting-defective larvae of other genotypes, which typically arrest development trapped in a single cuticle [10]. Consistent with this finding, *lin-42(ok2385)* mutants occasionally shed two cuticles within 1 to 2 hr during time courses (data not shown). Together, these observations suggest that some ecdyses occurred at unusually short, rather than unusually long, intervals in *lin-42(ok2385)* mutants. Thus, *lin-42a* is essential for rapid larval development and the timely execution of molts.

lin-42 Is Continuously Required for Seam Cell Development

The heterochronic gene regulatory network, which includes *lin-42*, programs successive transitions in the temporal fate of the epidermis, which result in stage-specific patterns of cell division, differentiation, and fusion [16]. Briefly, the lateral seam cells undergo stem-cell-like asymmetric divisions early in every larval stage. The anterior daughters fuse with the major body hypodermal syncytium (hyp7), whereas the posterior daughters retain the seam cell fate [18]. The seam cells separate from one another prior to dividing in the L1-stage; the posterior daughters then elongate over the hypoderm and connect to one another prior to the first molt [27]. Dynamic changes in cell shape and connectivity also accompany the asymmetric divisions in later larval stages. During the larval-to-adult transition, the seam cells terminally differentiate, exit the cell cycle, fuse into two lateral syncytia, and secrete longitudinal ridges (alae) characteristic of adult-stage cuticles [19].

Molecular mechanisms that synchronize progressive transitions in the temporal fates of seam cells with the periodic molts have not been well characterized. The *lin-42* gene was previously known to program the temporal fate of the seam cells at the L3 stage; in other *lin-42* mutants, the seam cells fuse and secrete adult-specific alae precociously during the third molt [22, 28]. To determine the extent to which *lin-42* is required for proper specification of the epidermis during other life stages, we visualized and compared the seam cells and syncytia of *lin-42(ok2385)* mutants and wild-type animals throughout development, using the AJM-1::GFP fusion protein to detect adherens junctions at the seam cell margins and the *scm::gfp* reporter to detect seam nuclei [29]. Gross abnormalities in cell shape and connectivity were observed in most *lin-42(ok2385)* mutants undergoing each of the four molts (Figures 3A–3C). In the late L1 and L2 stages, large gaps devoid of AJM-1::GFP were observed among seam nuclei of *lin-42(ok2385)* mutants, in addition to atypical, small rings of AJM-1::GFP that did not surround *scm::gfp*+ nuclei. Four or more distinct gaps were observed in 42% (n = 46) of mutants undergoing the first molt. This set included 14 selected mutants that began to molt at the standard time (16 hr). Thus, the gaps did not result from delay of the molt per se (Figure 3B). Instead, aberrant cell behavior during the L1 stage likely accounted for the gaps, because the seam cells were properly connected in *lin-42(ok2385)* hatchlings (Figure S3A).

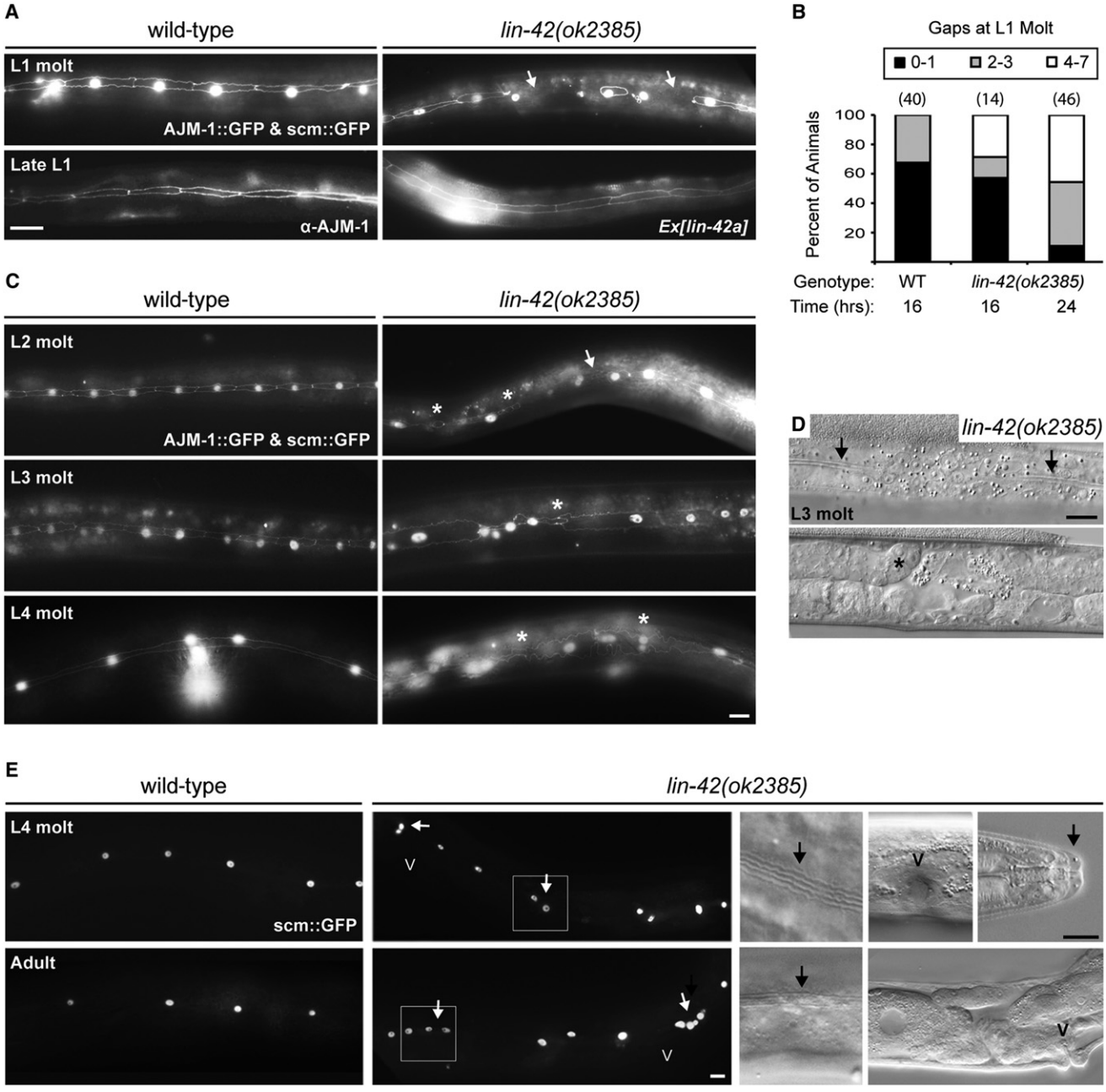

Figure 3. Continuously Abnormal Seam Cell Development in *lin-42(ok2385)* Mutants

(A) Upper panels show representative fluorescence micrographs of the seam nuclei and adherens junctions, marked by *scm::gfp* and AJM-1::GFP, respectively. Arrows indicate gaps between seam cells in *lin-42(ok2385)* mutants undergoing the first molt. Lower panels show interconnected seam cells of wild-type and *aaaEx30[lin-42a] lin-42(ok2385)* larvae stained with anti-AJM-1 antibodies.

(B) Graph shows the proportion of larvae with 0–1, 2–3, or 4–7 distinct gaps among the seam cells. Molting larvae were selected based on the presence of cuticle caps over the mouth. Sample sizes are indicated in parentheses.

(C) Malformation of seam cells and syncytia in *lin-42(ok2385)* mutants undergoing subsequent molts. Arrows indicate gaps between seam cells. Asterisks indicate misshapen structures labeled by AJM-1::GFP.

(D) Precocious formation of discontinuous alae (arrows) in a representative *ok2385* larva undergoing the third molt. The fully turned gonad (*) and lack of vulval invagination evident in the lower DIC image were characteristic of *lin-42* mutants at this stage.

(E) Pairs of seam nuclei (white arrows) in L4-molt and adult-stage *lin-42(ok2385)* animals. Corresponding DIC images show alae (black arrows) above the boxed regions. Additional images of the vulva (V) and L4-cuticle cap (black arrow) confirm the stage of the animals. Scale bars represent 10 μm.

In addition, the first seam cell divisions began contemporaneously in *lin-42(ok2385)* mutants and wild-type larvae, as indicated by simultaneous increases in the numbers of *scm::gfp*+ nuclei (Figure S3B). Most *lin-42(ok2385)* mutants therefore began the L1 molt later than wild-type larvae, relative to the time of seam cell divisions. Nevertheless, the mutants molted while many seam cells were not connected. In this context, the first molt was uncoupled from seam cell dynamics in

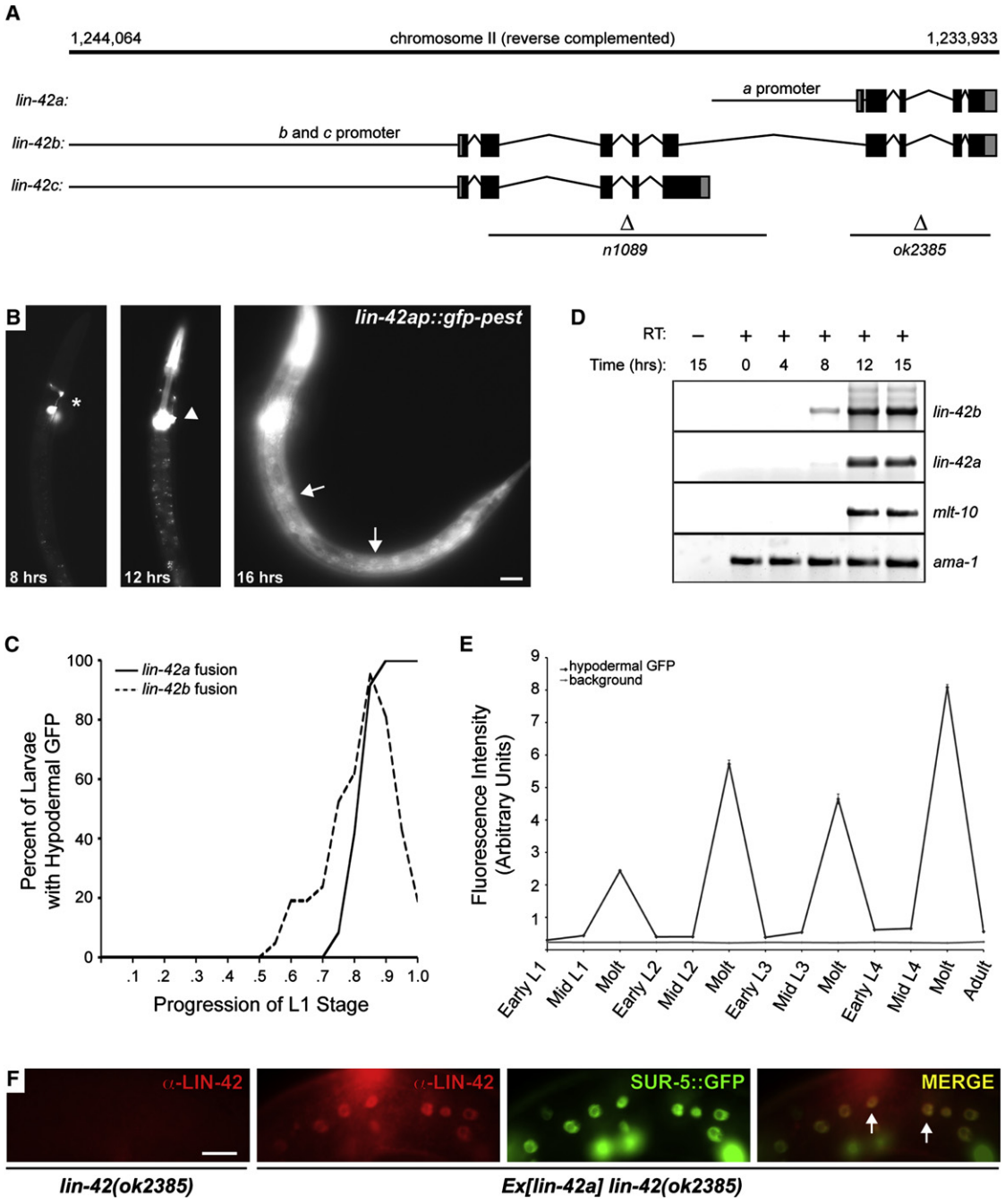

Figure 4. Temporally Reiterated Expression of the *lin-42a* Isoform Coincides with Molts

(A) Gene models for the three major isoforms of *lin-42* annotated in WS227. Black boxes represent exons; gray boxes represent untranslated sequences. The position and size of the *ok2385* and *n1089* deletions and sequences used to construct *lin-42a* and *lin-42b/c* transcriptional fusion genes are represented. Accession numbers for the *lin-42* isoforms are as follows: *a*, NM_001027005; *b*, NM_001027006; and *c*, NM_001027007. Tennessen and colleagues previously described these three isoforms as *lin-42d*, *lin-42c*, and *lin-42a*, respectively, and identified a fourth transcript (*lin-42b*) by rapid amplification of complementary DNA (cDNA) ends (RACE) [23]. Nucleotide positions correspond to *C. elegans* chromosome II (gi|212645681).

(B–E) Larvae were synchronized in starvation-induced L1-diapause and then fed and cultivated at 25°C for the indicated times.

(B) Representative fluorescence images show expression of the *lin-42ap::gfp-pest* reporter in the pharynx (arrowhead) and lateral hypodermis (arrows). The larva imaged at 16 hr was molting and had a cuticle cap over the mouth. The asterisk indicates GFP expressed in AIY neurons from the cotransformation marker *ttx-3p::gfp*.

(C) Frequency of GFP expression in the hypodermis of *Ex[lin-42ap::gfp-pest]* and *Ex[lin-42bp::gfp-pest]* larvae throughout the L1 stage. By definition, time 0 corresponded to release from starvation and time 1.0 corresponded to ecdysis, for every larva observed. n = 12 for *Ex[lin-42ap::gfp-pest]* larvae; n = 21 for *Ex[lin-42bp::gfp-pest]* larvae.

(D) Detection of *lin-42a* and *lin-42b* transcripts expressed in wild-type larvae by RT-PCR. Amplification of *mlt-10* cDNAs provided an internal benchmark for the first molt. Detection of *ama-1* transcripts controlled for sample quality and equivalent loading of PCR products.

(E) Expression of *lin-42ap::gfp-pest* cycles throughout larval development. The intensity of fluorescence in transgenic larvae was measured using the quantitative image analysis software Volocity. For each time point, values indicate the mean pixel intensity (±SEM) of 12–27 distinct objects (areas $\geq$ 50 μm^2)

lin-42(ok2385) mutants. This phenotype was attributable to loss of the *lin-42a* isoform, because *aaaEx30[lin-42a]* was sufficient to restore proper seam cell shape and connectivity to late L1-stage *lin-42(ok2385)* mutants (Figure 3A). The normal coordination between maturation of the vulva and completion of the fourth molt was also disrupted in *lin-42(ok2385)* mutants; the lumen of the vulva had often not collapsed by the time of ecdysis (Figure S3C). The cause of this defect in vulval development is not yet known.

Further characterization of the seam cells indicated that *lin-42(ok2385)* mutants exhibited a novel phenotype that combined features of so-called "precocious" and "retarded" heterochronic mutants. Some seam cells were fused with one another in *lin-42(ok2385)* mutants undergoing the third molt, as previously described for *lin-42(n1089)* and *lin-42(ve11)* mutants [22, 28]. The related precocious synthesis of adult-specific alae was observed in 100% (n = 13) of *lin-42(ok2385)* mutants (Figure 3D). Nevertheless, closely positioned pairs of *scm::gfp*+ seam nuclei were observed in *lin-42(ok2385)* mutants during the L4 molt and the young adult stage; in some instances, the paired nuclei were seen pulling apart from one another (Figure 3E). On average, 18.2 ± 0.7 (SEM, n = 15) *scm::gfp*+ nuclei were detected in *lin-42(ok2385)* mutants undergoing the L4 molt, compared with 16.1 ± 0.1 (n = 13) in wild-type larvae; 18.1 ± 0.4 (n = 14) nuclei were detected in *lin-42(ok2385)* young adults, compared with 16.0 ± 0 (n = 6) in wild-type animals. These observations strongly suggest that some seam nuclei failed to exit the cell cycle at the larval-to-adult transition and instead underwent supernumerary divisions in *lin-42(ok2385)* mutants. Based on the aforementioned phenotypes, we conclude that *lin-42* is continuously required for proper postembryonic development of the epidermis, as well as the timing and execution of rhythmic molts. The combination of stage-specific and reiterative actions of LIN-42 may coordinate these distinct but interdependent processes. In any case, our findings extend the role of *lin-42* in seam cell development formerly established by studies of mutations that did not completely abrogate expression of the *lin-42a* isoform [22].

The *C. elegans nhr-25* gene, which is homologous to *Drosophila melanogaster FTZ-f1* and mammalian *SF-1*, likewise regulates both seam cell dynamics and molting cycles [30–33] and interacts genetically with several components of the heterochronic pathway [20, 34]. Further, expression of *nhr-25* in the epidermis cycles in phase with the larval molts [35]. We therefore hypothesized that NHR-25 acts as an auxiliary component of the molting cycle timer. Consistent with that idea, RNA interference (RNAi) of *nhr-25* enhanced the developmental delay and molting defects associated with *lin-42(ok2385)*, to the extent that nearly half of the mutants became trapped in the L1- or L2-stage cuticle and none became adults within 78 hr of cultivation (Figure S4A). The conditional *nhr-25(ku217)* mutation also augmented the adverse effect of forced *lin-42a* expression (Figure S4B). In addition, *nhr-25(ku217)* mutants cultivated continuously at the restrictive temperature of 25°C developed very slowly; 63% (n = 43) of the mutants failed to complete the first molt after 96 hr of cultivation (Figure S4C). These genetic interactions are consistent with the model that LIN-42A and NHR-25 sustain the pace and productivity of molting cycles through partly parallel pathways.

Expression of *lin-42a* in the Epidermis Peaks during Every Molt

Because genetic analysis identified *lin-42a* as critical for the progression of molting cycles, we further characterized the temporal and spatial expression pattern of the *lin-42a* isoform. The presence of both common and distinct regulatory elements in *lin-42a*, *lin-42b*, and *lin-42c* transcripts indicated that the corresponding proteins might be expressed in overlapping but nonidentical patterns (Figure 4A). In particular, the unique 5′ UTR found in *lin-42a* complementary DNAs (cDNAs) suggested that *lin-42a* was transcribed separately from *lin-42b* and *lin-42c*, rather than alternatively spliced from a common precursor. However, reagents previously used to characterize the expression pattern of *lin-42* transcripts and proteins did not distinguish between *lin-42a* and *lin-42b* [22, 23].

To characterize the dynamic expression of *lin-42a* during larval development, we fused the predicted promoter of *lin-42a* with the *gfp-pest* reporter, which encodes a variant of GFP with a half-life of approximately 1 hr in vivo [10]. For comparison, we constructed a similar fusion gene between the shared promoter of *lin-42b* and *lin-42c* and *gfp-pest.* GFP expressed from the *lin-42a* promoter was robustly expressed in the pharyngeal myoepithelium midway through the L1 stage and continuously thereafter (Figure 4B). The *lin-42a* reporter was also expressed in hyp7 and the lateral seam cells of late L1-stage larvae undergoing the first molt (Figure 4B). Expression of the *lin-42a* reporter in the hypodermis was detected later in the L1 stage than expression of the *lin-42b* reporter. Fluorescence from the *lin-42a* reporter also persisted through ecdysis, whereas fluorescence from the *lin-42b* reporter dissipated during lethargus (Figure 4C). As a complementary approach to resolve the temporal expression patterns of *lin-42a* and *lin-42b*, we used semiquantitative RT-PCR to detect transcripts of both isoforms in wild-type larvae collected at regular intervals after release from starvation-induced L1 diapause. As expected, transcripts of *lin-42a* were detected later than transcripts of *lin-42b* (Figure 4D). These observations confirmed that the shared promoter of *lin-42b* and *lin-42c* was most active during the intermolt, as previously reported [22]. However, the unique promoter of *lin-42a*, which was defined through this analysis, was most active late in the L1 stage, during the first molt. GFP from the *lin-42ap::gfp-pest* reporter was likewise detected in the hypodermis of 100% (n = 39) of lethargic larvae undergoing the subsequent molts.

To fully define the cyclical expression pattern of the *lin-42ap::gfp-pest* fusion gene, we measured the relative intensity of the associated fluorescence in the hypodermis throughout larval development. For this analysis, animals were collected and imaged early, midway, and late in every larval stage; molting larvae were identified by the presence of cuticle caps over the buccal cavity. The intensity of fluorescence repeatedly increased 2- to 10-fold during the molts and

within the lateral hypodermis of 4–9 different larvae. Early and midstage larvae were selected from partly synchronized populations, based on gonad development and body size. Molting larvae were selected based on the presence of cuticle caps over the mouth.

(F) Detection of LIN-42A (red) in hypodermal nuclei of late L4-stage animals by immunofluorescence microscopy using anti-LIN-42A/B primary antibodies. In *aaaEx30[lin-42a sur-5::gfp] lin-42(ok2385)* larvae, nuclear fluorescence from SUR-5::GFP was also detected. Arrows mark examples of LIN-42A-positive hypodermal nuclei. Scale bars represent 10 μm.

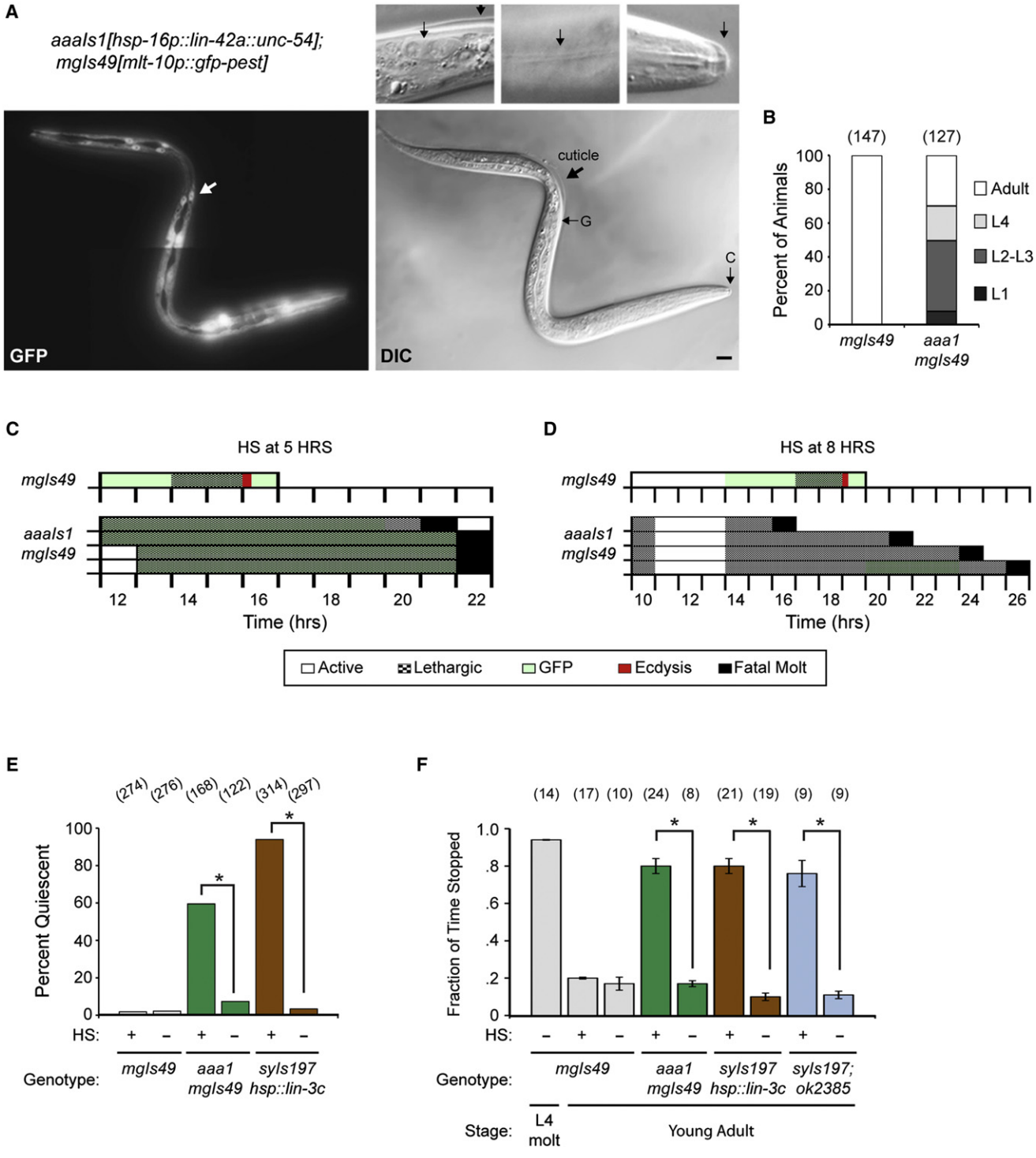

Figure 5. Forced Expression of *lin-42a* Results in Anachronistic Molts and Lethargy

(A–D) Early L1 larvae were synchronized by starvation-induced diapause and then fed and cultivated at 25°C. Animals were subjected to an acute HS 5 (A–C) or 8 (D) hr after release from starvation.

(A) Fluorescence and DIC images show a representative *aaaIs1;mgIs49* larva undergoing an anachronistic molt after 30 hr of cultivation. White arrow indicates expression of the *mlt-10p::gfp-pest* fusion gene in hyp7. Thick black arrow indicates separation of the cuticle from the body. Only two nuclei were detected in the gonad (G). Digitally magnified images show the gonad, L1-specific alae on the outer cuticle, and a cuticle cap (C) covering the mouth. Scale bar represents 10 μm.

(B) Distribution of animals among larval and adult stages after 52 hr of cultivation, as determined by visual inspection. Sample sizes are indicated in parentheses.

(C and D) Each bar depicts expression the *mlt-10p::gfp-pest* reporter, as well as the behavior and development of a single larva, as described for Figure 2. (C) Fluorescent larvae were selected at the start of this time course. The life histories of *aaaIs1* larvae that were inactive for extended periods, expressed GFP, and perished in aberrant molts are depicted, compared with a representative *mgIs49* larva.

dropped to background levels early in the next life stage (Figure 4E). Immunostaining of *aaaEx30[lin-42a] lin-42(ok2385)* animals with anti-LIN-42A/B antibodies [23] confirmed the presence of LIN-42A in hypodermal nuclei of late L4-stage larvae (Figure 4F); the antigen was detected in 41% (n = 41) of *aaaEx30* larvae, and 0% (n = 14) of nontransgenic siblings. Taken together, these observations indicate that rising and falling levels of LIN-42A coincide, respectively, with the start and completion of every molt.

To define the site of *lin-42a* action critical for regular molting cycles, we fused the coding sequence of *lin-42a* with the promoter of either *nhr-72* or *myo-2*, and the 3′ UTR of *unc-54*. The *nhr-72* and *myo-2* promoters drive gene expression in the seam cells and pharynx, respectively, throughout larval development [36, 37]. The *nhr-72p::lin-42a::unc-54* fusion gene restored the rapid pace of the L4-stage (Figure 1B) and completion of the fourth molt in *lin-42(ok2385)* mutants. In contrast, the *myo-2p::lin-42a::unc-54* fusion gene exacerbated the developmental delay of *lin-42(ok2385)* mutants (Figure 2B) and rendered 65% (n = 20) of the mutants unable to shed the L1-stage cuticle. The inability of this particular fusion gene to rescue *ok2385* mutants could be attributable to either the spatial or temporal pattern of expression of *lin-42a* from the *myo-2* promoter. Nonetheless, these observations identify the lateral seam cells as a major site of action of the LIN-42-based molting cycle timer.

Forced Expression of *lin-42a* Leads to Anachronistic Larval Molts and Lethargy

As a complementary approach to evaluate the function of *lin-42a*, we characterized the effect of *lin-42a* overexpression (OE) on the rhythmic cellular and animal behaviors associated with molting cycles (Figure 5). The coding sequence of *lin-42a* was fused with the *hsp-16-41* promoter, which is activated by heat shock (HS) in most somatic tissues, and the *unc-54* 3′ UTR, which is not targeted by the *let-7* family of miRNAs [38]. In contrast, the endogenous 3′ UTR of *lin-42a* and *lin-42b* contains predicted *let-7* binding sites that may trigger gene silencing [21]. The corresponding integrated array, *aaaIs1[hsp-16p::lin-42a::unc-54]*, was not toxic to animals cultivated at 15°C. To evaluate the effect of forced, chronic expression of *lin-42a* on larval development, we heat-shocked early L1-stage *aaaIs1; mgIs49[mlt-10p::gfp-pest]* larvae 5 hr after release from starvation, isolated them, and cultivated them at 25°C. Under these conditions, particular larvae underwent anachronistic molts, in which the cuticle separated from the body prior to proliferation of the germline or growth of the body (Figure 5A). Some of these larvae expressed the GFP reporter for *mlt-10* and were lethargic for prolonged periods prior to an aberrant ecdysis (Figure 5C). However, the majority of *aaaIs1* animals did not express *mlt-10* in a timely fashion and did not complete larval development within 52 hr of cultivation; control animals became adults in that time (Figure 5B). In a complementary experiment, larvae were heat-shocked 8 hr after release from starvation; 10.3% (n = 368) of these larvae were inactive 2 hr after HS, compared with 0% (n = 222) of *mgIs49* larvae treated in the same manner. Twenty-four inactive *aaaIs1* larvae were isolated and monitored for an additional 18 hr. Three failed to express the *mlt-10p::gfp-pest* fusion gene but nevertheless attempted to shed to the L1 cuticle and perished (Figure 5D). Others underwent sporadic bouts of quiescence but failed to express the GFP reporter (Figure S5B). Likewise, a subset of early L1-stage larvae with the distinct, high-copy *aaaEx20[hsp-16::lin-42a::unc-54]* array began to molt just 2 hr after HS (Movie S1A). Taken together, these observations show that forced expression of *lin-42a* results in anachronistic larval molts and lethargy. These anachronistic molts were uncoupled from completion of characteristic L1-stage and possibly later stage-specific developmental events, unlinked from expression of the *mlt-10* reporter in some cases, executed at irregular times relative to release from L1-diapause, and typically fatal. The observation that chronic expression of *lin-42a* delayed or decreased expression of the *mlt-10* reporter in many *aaaIs1* larvae is consistent with prior studies in mammalian cells; constitutive expression of *mPER2* abrogates the rhythmic expression of clock-controlled genes normally expressed in phase with PER2 [39, 40]. Additional factors, including NHRs that are active during specific segments of every larval stage, are likely required to induce the expression of *mlt-10* and other cuticle components.

As a complementary approach to evaluate the physical activity of juveniles with excess LIN-42A, we measured the feeding rates of early L1-stage larvae (Figure S5C). The average pumping rate in *aaaEx20[hsp-16p::lin-42a::unc-54]* larvae 2 hr after HS was 17.1 ± 7.6 p/m (SEM, n = 24), compared with 183.2 ± 8.5 p/m (n = 11) for nontransgenic siblings. The *hsp-16p::lin-42a* array used in these experiments also reduced the pumping rate of mock-treated animals, likely due to constitutive expression of *lin-42a*.

The sleep-like behavioral quiescence associated with molting is regulated both by LIN-3/EGF (epidermal growth factor)-like signaling in the ALA neuron and the EGL-4 cyclic guanosine monophosphate-dependent protein kinase [13, 14]. To determine the extent to which the cessation of feeding associated with the *hsp-16p::lin-42a* fusion gene depended on these signaling pathways, we also measured the pumping rates of *aaaEx20 ceh-14(ch3)* and *aaaEx20 egl-4(n479)* larvae. The *ceh-14* mutation blocks LIN-3/EGF-induced quiescence; the *egl-4(n479)* mutation inhibits locomotory quiescence. Both of these mutations significantly increased the feeding rate of *aaaEx20* larvae, but neither mutation fully suppressed the effect of the array, particularly after HS (Figure S5C). These results do not order *lin-42a* relative to *lin-3* or *egl-4* in a genetic pathway, but nonetheless suggest that neuroendocrine signaling contributes to the reduced feeding of *aaaEx20* larvae. Subtle anatomical defects in the pharynx may also contribute to this behavioral phenotype.

We further determined the effect of forced expression of *lin-42a* on the behavior of adults, which had completed all four standard molts. Animals were cultivated at 25°C, heat-shocked as young adults, permitted to recover for 4 hr, and

(D) Quiescent *aaaIs1* larvae were selected at the start of this time course. The life histories of larvae that were inactive for extended periods, expressed little or no GFP, and perished in aberrant molts are depicted, compared with a representative *mgIs49* larva. Life histories of other larvae observed in these experiments are shown in Figures S5A and S5B.

(E) Frequency of behavioral quiescence in young adults 4 hr after an acute heat shock. Values represent the weighted average from three independent trials. *p < 0.001, chi-square test.

(F) Quiescent *aaaIs1* adults and control animals did not exhibit locomotion for the indicated fractions of three 60 s intervals. Values represent the mean (±SEM) from two to three independent trials. *p < 0.001, Student's t test. Samples sizes are indicated in parentheses.

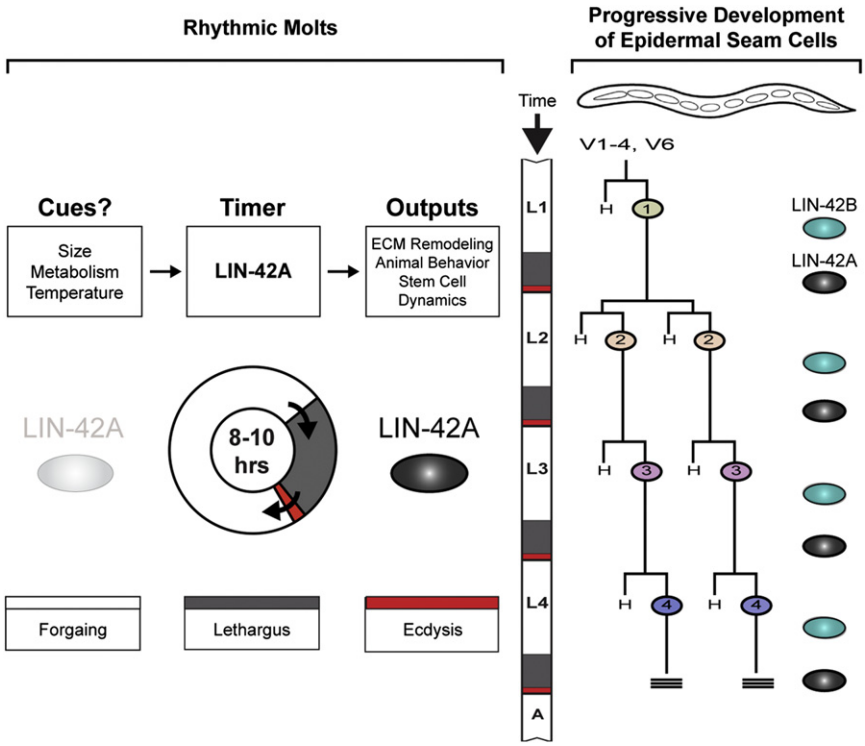

Figure 6. Model for the Temporal Regulation of Molting Cycles and Epidermal Development by LIN-42

We propose that rising and falling levels of LIN-42A allow the start and completion of molting, respectively. Conserved nuclear hormone receptors might act as auxiliary components of the molting cycle timer. Physiological and environmental conditions likely modulate the reiterative function(s) of LIN-42. The rhythmic expression of LIN-42A and LIN-42B in the lateral seam cells is also depicted; this expression pattern almost certainly relates to the requirement for *lin-42* in seam cell development. Overall, LIN-42A and additional factors may control rhythmic cellular and animal behaviors underlying the larval molts, similar to the way in which PERIOD (PER)-based oscillators drive rhythmic behaviors and metabolic processes in mature animals. Further, reiterative and stage-specific functions of LIN-42/PER may coordinate periodic molts with progressive transitions in the temporal fates of epidermal cells. H refers to hyp7. Triple bars denote seam cell fusion and production of adult-specific alae.

then observed by light microscopy. Behavioral quiescence was indicated by a lack of detectable locomotion or pharyngeal contractions within 10 s of observation. Sixty percent (n = 168) of *aaaIs1* animals became quiescent, compared with 2% (n = 274) of control animals (Figure 5E). On average, those *aaaIs1; mgIs49* adults scored as quiescent were immobile for 80% ± 16 (SEM, n = 24) of three 60 s intervals, whereas *mgIs49* adults were immobile for 20% ± 0.5 (n = 17) (Figure 5F). Notably, quiescent *aaaIs1* adults responded to UV light with vigorous aversive movements (Movie S1B), confirming that the behavioral state was reversible and not attributable to gross deformities of the musculature or hypoderm. LIN-3/EGF-induced quiescence provided a positive control for these experiments [14]. Consistent with the model that LIN-3 acts either in parallel or downstream of LIN-42A, forced expression of LIN-3 induced behavioral quiescence in both *lin-42(ok2385)* mutants and wild-type adults (Figure 5F). We conclude that *lin-42a(OE)* results in anachronistic lethargy in both juvenile and adult nematodes. This finding is consistent with studies in mice; forced expression of PER results in sporadic bouts of physical activity that are uncoupled from external light/dark cycles [40]. Collectively, our findings indicate that forced expression of *lin-42a* uncouples the rhythmic behaviors and cell biological processes characteristic of molting cycles from animal development. This result implies that oscillatory expression of *lin-42a* is critical for postembryonic development.

Discussion

In summary, we find that the *period*-like, heterochronic gene *lin-42a* of *C. elegans* is required for rapid, rhythmic, and productive molting cycles, as well as the continuous postembryonic development of epidermal stem cells and related syncytia. The oscillatory expression of the *lin-42a* transcriptional reporter peaks during all four molts. Moreover, forced expression of *lin-42a* results in anachronistic larval molts and lethargy. Based on these findings, we propose that rising and falling levels of LIN-42A allow the start and completion of molting cycles, respectively (Figure 6). Reiterated actions of LIN-42A/PER may orchestrate rhythmic cellular and animal behaviors critical for productive molts. Transcriptional regulation of numerous downstream target genes likely affects the timing of key steps in the molting cycle. The aberrant ecdyses associated with *lin-42(ok2385)* may therefore result from improper coordination of earlier events in the molt. Consistent with that view, forced expression of *lin-42a* also resulted in mistimed and fatal ecdyses. Alternatively, a specific level of LIN-42A activity may be required for ecdysis. Overall, LIN-42A and auxiliary factors may regulate molting cycles in much the same way that PER-based oscillators control rhythmic behaviors and metabolic processes in mature insects and mammals [1].

The significance of the LIN-42A isoform suggests that the SYQ and LT sequence motifs, which are conserved between LIN-42A and human PER1, perform distinct functions from the PAS domain. However, all three isoforms of *lin-42* may interact genetically or biochemically and influence the pace of larval development under physiologic conditions. As described, excess *lin-42c* dramatically reduced the pace of development in *lin-42(ok2385)* larvae, suggesting that LIN-42A might normally antagonize the activity of LIN-42C. On the other hand, LIN-42A and LIN-42B might perform partly redundant functions related to the SYQ and LT motifs. Considering the structure of the locus, it is also possible that the cyclical expression of *lin-42a* might depend, in part, on the rhythmic expression of *lin-42b*. In theory, PAS domain-mediated interactions among LIN-42B and LIN-42C might affect expression of those isoforms, similar to how PAS domain-mediated homodimerization modulates the rhythmic expression of *Drosophila* PER [41]. In any case, further studies of LIN-42A and the molting cycle timer may uncover new mechanisms by which PER-based oscillators control essential rhythmic processes in metazoan development.

Our findings further suggest that the stage-specific and temporally reiterated actions of *lin-42* coordinate progressive transitions in the temporal fates of epidermal seam cells with periodic molts (Figure 6). As described, the seam cells of *lin-42(ok2385)* mutants behave abnormally during every larval stage. Many seam cells fail to reconnect prior to the first molt. The seam cells also fuse prematurely and produce adult-specific alae during the L3 molt. Nevertheless, some seam cells appear to undergo extra rounds of division during the L4 molt and the adult stage. This phenotype combines classic features of "retarded" and "precocious" heterochronic mutants. In theory, recurrent actions of LIN-42 during the molts may enable temporal respecification of the seam cells, as appropriate for the upcoming, rather than the passing, life-stage. Consistent with this idea, results emerging in the field suggest that *lin-42* regulates the expression of small temporal RNAs including *let-7* throughout development (Amy Pasquinelli, UCSD, personal communication).

Seam cell dynamics and molting are interdependent processes, in part because seam cells and syncytia contribute to the synthesis of new cuticles. Accordingly, both genetic mutations that block seam cell specification and drugs that delay the completion of seam cell divisions cause aberrant ecdyses [42, 43]. Further, intercellular signaling among seam cells, neurons, and muscles may regulate the distinctive animal behaviors that accompany ECM remodeling and ecdysis. Indeed, DOS (Delta and OSM-11)-motif signaling proteins secreted from the seam cells regulate the lethargy associated with molting, by activating Notch receptors in the nervous system [15]. Finding that expression of *lin-42a* in the seam cells was sufficient to restore rhythmic molting behaviors further supports this view. In addition, mutations in *lin-42* have been reported to alter circadian rhythms in the locomotor activity of adult *C. elegans* [44].

The combined use of reiterative and stage-specific functions of LIN-42/PER to program rhythmic and successive behaviors of epidermal cells may represent a widespread paradigm for the integration of cyclical and progressive processes in metazoan development. Related timing mechanisms likely operate in other phyla; mutations in *per* alter the pace of larval development in *Drosophila*, and circadian clocks gate eclosion in many insect species [45, 46]. Moreover, the counterparts of several heterochronic genes regulate developmental timing in diverse organisms [47, 48].

The best-characterized biological oscillators of mammals are composed of interconnected positive and negative regulatory feedback loops among PER, the transcriptional activators CLOCK and BMAL, the NHR RORα, and additional factors [1]. *C. elegans* NHR-23/RORα, NHR-25/SF-1, or DAF-12/VDR might likewise serve as auxiliary components of the molting cycle timer. Indeed, genetic analyses indicate that LIN-42A and NHR-25 control the pace of development and execution of the larval molts through partially parallel pathways. In theory, transcriptional activation of the *let-7* miRNA by ligand-bound DAF-12 [49, 50] and posttranscriptional inhibition of the *lin-42*, *nhr-25*, and *daf-12* genes by the *let-7* family [20, 21] could generate regulatory loops that fine-tune the rhythm of molting cycles. The discovery that expression of primary *let-7* transcripts cycles in phase with the molts is consistent with this idea [51]. However, the gene regulatory networks that control the oscillatory expression of *lin-42*, *nhr-23* and *-25*, and *let-7* have not yet been defined.

PER-based clocks in other systems synchronize biological rhythms with predictable fluctuations in intrinsic and extrinsic conditions. The proposed molting cycle timer may also be responsive to physiological and environmental cues. Both the size of shed cuticles and the rate of larval growth increase incrementally at successive molts [52, 53], suggesting that larvae molt at critical sizes. Further, because the buccal cavity enlarges saltationally at the molts, whereas the body grows continuously [53], molts may coincide with recurrent fluctuations in the nutritional status of the organism. Consistent with this view, the insulin-signaling pathway is known to affect the pace of larval development [54]. In addition, rhythmic fluctuations in ambient temperature can entrain the oscillatory expression of several *C. elegans* genes that act in molting cycles [55]. This phenomenon is noteworthy because temperature affects the pace of larval development, whereas circadian clocks are temperature compensated [1]. In theory, endocrine signaling linked to body size, metabolism, or ambient temperature may impinge on the reiterative functions of LIN-42 and the irreversible commitment to molt [24].

The finding that genetic alterations that abrogate the cycling of *lin-42* deregulate the onset and duration of quiescent episodes in both larvae and adults further supports the model of a common evolutionary origin for nematode lethargus and vertebrate sleep [13, 14]. Further studies of the molting cycle timer may therefore uncover novel but conserved aspects of the biological clocks underlying sleep-wake cycles and metabolic rhythms in more complex animals.

Experimental Procedures

Genetics and Molecular Biology

The culture and genetic manipulation of *C. elegans* were performed using standard methods [56]. The strains generated and used in this report are fully described in Supplemental Experimental Procedures. Sequences of PCR primers are available upon request. To amplify transcripts of specific isoforms of *lin-42* and other genes, we extracted total RNA from nematodes as previously described [48]. TURBO and RETROSCRIPT kits (Ambion) were then used to remove contaminating genomic DNA and synthesize cDNAs, respectively. All PCR reactions were conducted with Phusion High-Fidelity Polymerase (Finnzymes) and products confirmed by sequencing as needed. The genomic DNA fragments in *aaaEx30[lin-42a]* and *aaaEx34[lin-42c]* correspond to nucleotides 1233956–1239528 and 1239373–1249503 of *C. elegans* chromosome II (gi|212645681), respectively. To construct the *lin-42ap::gfp-pest* reporter gene, we fused the start codon of *lin-42a* and 3,043 bps of upstream sequence with *gfp-pest*; the comparable *lin-42b/c* reporter contains the start codon and 5,490 bps of upstream sequence. To construct the *hsp-16p::lin-42a::unc-54* fusion gene, we isolated *lin-42a* cDNAs by RT-PCR and cloned them into pPD49_83 (Fire Lab), generating plasmid pGM3. The integrated array *aaaIs1[hsp-16p::lin-42a::unc-54]* was derived by UV irradiation of *aaaEx21* animals. All strains harboring the *hsp-16p::lin-42a::unc-54* fusion gene were routinely cultivated at 15°C to repress activity of the *hsp-16* promoter. Prior to characterization, *aaaIs1*, *lin-42(ok2385)*, and *nhr-25(ku217)* were out-crossed three times to KP3913 or N2 animals to remove unlinked mutations in the background. To construct the *myo-2p::lin-42a::unc-54* fusion gene, we cloned *lin-42a* cDNAs into pPD30_69 (Fire Lab), generating pGM9. To make the *nhr-72p::lin-42a::unc-54* fusion gene, we amplified nucleotides 3850433–3853432 of *C. elegans* chromosome II and used them to replace the *hsp-16* promoter in pGM3. Corresponding arrays were generated by injecting N2 animals with mixtures that contained 10 ng/μl of the recombinant plasmids in a total of 100 ng/μl DNA.

Developmental and Behavioral Assays

To track the behavior and developmental progress of animals of various genotypes, we transferred individual larvae to nematode growth medium (NGM) plates seeded with 10 μl of *E. coli* OP50, cultivated at 25°C, and repeatedly observed for 30 s of every hr using a Zeiss M^{2}BioDiscovery microscope at 300- to 1,000-fold magnification. After scoring behavior, expression of GFP from the *mlt-10p::gfp-pest*, *lin-42ap::gfp-pest*, or *lin-42b/cp::gfp-pest* fusion gene was assessed during 3 s of exposure to UV light. For measurements of feeding rates, larvae were subjected to acute

HS (33°C for 30 min) and allowed to recover at 15°C for 2 hr. Larvae were then transferred to NGM plates freshly seeded with 10 μl of OP50 and secured beneath a coverslip dampened with M9 buffer. Larvae in the L1 intermolt were selected based on the size of the body and gonad. Pharyngeal contractions were observed for 30 s using a Zeiss M^{2}BioDiscovery microscope and recorded using an attached Sony NDR-XR500V video camera at 12-fold optical zoom. The resulting videos were played back at half-speed using Quicktime Player Version 7.7. The pumps made by each larva were counted three independent times, blind to the genotype and experimental conditions; the consistency among counts was ≥93%. Average values were used for further comparisons and statistical analyses. For measurements of locomotory quiescence, young adults cultivated on concentrated OP50 were heat-shocked and allowed to recover for 4 hr. Individual animals were then observed for detectable locomotion during three 60 s intervals. The average time that a given animal was immobile was used in further analyses. The frequency of quiescent animals in corresponding populations was measured as described [15].

Immunofluorescence and Microscopy

Fixation of nematodes and immunostaining with MH27 monoclonal antibodies were performed as described [31]. Immunostaining with anti-LIN-42A/B polyclonal antibodies (1:10), provided courtesy of Ann Rougvie, and rhodamine-conjugated anti-rabbit secondary antibodies (1:400, Jackson Laboratories) was performed by the same method. Live animals were anesthetized with 30 mM sodium azide. Nematodes were observed using a Zeiss Axioscope and images captured with an attached Hamamatsu Orca ER camera controlled by the quantitative image analysis software package Volocity v5.5 (Improvision). Images were prepared for publication using Adobe Photoshop and Adobe Illustrator. To measure the relative intensity of expression of the *lin-42ap::gfp-pest* fusion gene, we selected animals at specific developmental stages from partially synchronized populations and corresponding fluorescent images captured with exposure times of 5, 50, and 200 ms. Three distinct objects with areas ≥50 μm^2 were selected within the lateral hypodermis of each larva, and the mean pixel intensity of each object was measured using Volocity; measurements were made from the brightest, nonsaturated image. For each time point, 12 to 27 distinct objects were measured in four to nine different larvae.

Supplemental Information

Supplemental Information includes five figures, Supplemental Experimental Procedures, and one movie and can be found with this article online at doi:10.1016/j.cub.2011.10.054.

Acknowledgments

The University of California Los Angeles School of Medicine supported this research, in addition to Ford Foundation and National Science Foundation Graduate Research Fellowships to G.C.M. Some *C. elegans* strains used in this study were provided by the Caenorhabditis Genetics Center. The Developmental Studies Hybridoma Bank provided the MH27 antibody. Ann Rougvie kindly provided anti-LIN-42 antibodies. We thank Tia Brandt, Ashish Sharma, and Jeffrey Matson for technical assistance. We are grateful to Paul Sternberg, Ann Rougvie, John Kim, Christopher Colwell, Cathy Clarke, and Alex Van der Bliek for helpful scientific discussions and critiques of this manuscript.

Received: March 7, 2011
Revised: October 7, 2011
Accepted: October 31, 2011
Published online: December 1, 2011

References

1. Bass, J., and Takahashi, J.S. (2010). Circadian integration of metabolism and energetics. Science *330*, 1349–1354.
2. Tomioka, K., and Matsumoto, A. (2010). A comparative view of insect circadian clock systems. Cell. Mol. Life Sci. *67*, 1397–1406.
3. Reid, K.J., and Zee, P.C. (2011). Circadian rhythm sleep disorders. Handb. Clin. Neurol. *99*, 963–977.
4. Gery, S., Komatsu, N., Baldjyan, L., Yu, A., Koo, D., and Koeffler, H.P. (2006). The circadian gene per1 plays an important role in cell growth and DNA damage control in human cancer cells. Mol. Cell *22*, 375–382.
5. McBrayer, Z., Ono, H., Shimell, M., Parvy, J.P., Beckstead, R.B., Warren, J.T., Thummel, C.S., Dauphin-Villemant, C., Gilbert, L.I., and O'Connor, M.B. (2007). Prothoracicotropic hormone regulates developmental timing and body size in Drosophila. Dev. Cell *13*, 857–871.
6. Rewitz, K.F., Yamanaka, N., and O'Connor, M.B. (2010). Steroid hormone inactivation is required during the juvenile-adult transition in Drosophila. Dev. Cell *19*, 895–902.
7. Thummel, C.S. (1996). Flies on steroids—Drosophila metamorphosis and the mechanisms of steroid hormone action. Trends Genet. *12*, 306–310.
8. Singh, R.N., and Sulston, J.E. (1978). Some observations on moulting in Caenorhabditis elegans. Nematologica *24*, 63–71.
9. Johnstone, I.L., and Barry, J.D. (1996). Temporal reiteration of a precise gene expression pattern during nematode development. EMBO J. *15*, 3633–3639.
10. Frand, A.R., Russel, S., and Ruvkun, G. (2005). Functional genomic analysis of C. elegans molting. PLoS Biol. *3*, e312.
11. Zaidel-Bar, R., Miller, S., Kaminsky, R., and Broday, L. (2010). Molting-specific downregulation of C. elegans body-wall muscle attachment sites: the role of RNF-5 E3 ligase. Biochem. Biophys. Res. Commun. *395*, 509–514.
12. Page, A.P., and Johnstone, I.L. (2007). The cuticle. WormBook, 1–15.
13. Raizen, D.M., Zimmerman, J.E., Maycock, M.H., Ta, U.D., You, Y.J., Sundaram, M.V., and Pack, A.I. (2008). Lethargus is a Caenorhabditis elegans sleep-like state. Nature *451*, 569–572.
14. Van Buskirk, C., and Sternberg, P.W. (2007). Epidermal growth factor signaling induces behavioral quiescence in Caenorhabditis elegans. Nat. Neurosci. *10*, 1300–1307.
15. Singh, K., Chao, M.Y., Somers, G.A., Komatsu, H., Corkins, M.E., Larkins-Ford, J., Tucey, T., Dionne, H.M., Walsh, M.B., Beaumont, E.K., et al. (2011). C. elegans Notch signaling regulates adult chemosensory response and larval molting quiescence. Curr. Biol. *21*, 825–834.
16. Moss, E.G. (2007). Heterochronic genes and the nature of developmental time. Curr. Biol. *17*, R425–R434.
17. Ambros, V., and Horvitz, H.R. (1984). Heterochronic mutants of the nematode Caenorhabditis elegans. Science *226*, 409–416.
18. Sulston, J.E., and Horvitz, H.R. (1977). Post-embryonic cell lineages of the nematode, Caenorhabditis elegans. Dev. Biol. *56*, 110–156.
19. Ambros, V. (1989). A hierarchy of regulatory genes controls a larva-to-adult developmental switch in C. elegans. Cell *57*, 49–57.
20. Hayes, G.D., Frand, A.R., and Ruvkun, G. (2006). The mir-84 and let-7 paralogous microRNA genes of Caenorhabditis elegans direct the cessation of molting via the conserved nuclear hormone receptors NHR-23 and NHR-25. Development *133*, 4631–4641.
21. Reinhart, B.J., Slack, F.J., Basson, M., Pasquinelli, A.E., Bettinger, J.C., Rougvie, A.E., Horvitz, H.R., and Ruvkun, G. (2000). The 21-nucleotide let-7 RNA regulates developmental timing in Caenorhabditis elegans. Nature *403*, 901–906.
22. Jeon, M., Gardner, H.F., Miller, E.A., Deshler, J., and Rougvie, A.E. (1999). Similarity of the C. elegans developmental timing protein LIN-42 to circadian rhythm proteins. Science *286*, 1141–1146.
23. Tennessen, J.M., Gardner, H.F., Volk, M.L., and Rougvie, A.E. (2006). Novel heterochronic functions of the Caenorhabditis elegans period-related protein LIN-42. Dev. Biol. *289*, 30–43.
24. Tennessen, J.M., Opperman, K.J., and Rougvie, A.E. (2010). The C. elegans developmental timing protein LIN-42 regulates diapause in response to environmental cues. Development *137*, 3501–3511.
25. Meli, V., Osuna, B., Ruvkun, G., and Frand, A.R. (2010). MLT-10 defines a family of DUF644 and proline-rich repeat proteins involved in the molting cycle of Caenorhabditis elegans. Mol. Biol. Cell *21*, 1648–1661.
26. Kostrouchova, M., Krause, M., Kostrouch, Z., and Rall, J.E. (2001). Nuclear hormone receptor CHR3 is a critical regulator of all four larval molts of the nematode Caenorhabditis elegans. Proc. Natl. Acad. Sci. USA *98*, 7360–7365.
27. Podbilewicz, B., and White, J.G. (1994). Cell fusions in the developing epithelial of C. elegans. Dev. Biol. *161*, 408–424.
28. Abrahante, J.E., Miller, E.A., and Rougvie, A.E. (1998). Identification of heterochronic mutants in Caenorhabditis elegans. Temporal misexpression of a collagen:green fluorescent protein fusion gene. Genetics *149*, 1335–1351.
29. Mohler, W.A., Simske, J.S., Williams-Masson, E.M., Hardin, J.D., and White, J.G. (1998). Dynamics and ultrastructure of developmental cell fusions in the Caenorhabditis elegans hypodermis. Curr. Biol. *8*, 1087–1090.

30. Gissendanner, C.R., and Sluder, A.E. (2000). nhr-25, the Caenorhabditis elegans ortholog of ftz-f1, is required for epidermal and somatic gonad development. Dev. Biol. *221*, 259–272.
31. Chen, Z., Eastburn, D.J., and Han, M. (2004). The Caenorhabditis elegans nuclear receptor gene nhr-25 regulates epidermal cell development. Mol. Cell. Biol. *24*, 7345–7358.
32. Asahina, M., Ishihara, T., Jindra, M., Kohara, Y., Katsura, I., and Hirose, S. (2000). The conserved nuclear receptor Ftz-F1 is required for embryogenesis, moulting and reproduction in Caenorhabditis elegans. Genes Cells *5*, 711–723.
33. Asahina, M., Valenta, T., Silhankova, M., Korinek, V., and Jindra, M. (2006). Crosstalk between a nuclear receptor and beta-catenin signaling decides cell fates in the C. elegans somatic gonad. Dev. Cell *11*, 203–211.
34. Hada, K., Asahina, M., Hasegawa, H., Kanaho, Y., Slack, F.J., and Niwa, R. (2010). The nuclear receptor gene nhr-25 plays multiple roles in the Caenorhabditis elegans heterochronic gene network to control the larva-to-adult transition. Dev. Biol. *344*, 1100–1109.
35. Gissendanner, C.R., Crossgrove, K., Kraus, K.A., Maina, C.V., and Sluder, A.E. (2004). Expression and function of conserved nuclear receptor genes in Caenorhabditis elegans. Dev. Biol. *266*, 399–416.
36. Miyabayashi, T., Palfreyman, M.T., Sluder, A.E., Slack, F., and Sengupta, P. (1999). Expression and function of members of a divergent nuclear receptor family in Caenorhabditis elegans. Dev. Biol. *215*, 314–331.
37. Ardizzi, J.P., and Epstein, H.F. (1987). Immunochemical localization of myosin heavy chain isoforms and paramyosin in developmentally and structurally diverse muscle cell types of the nematode Caenorhabditis elegans. J. Cell Biol. *105*, 2763–2770.
38. Didiano, D., and Hobert, O. (2008). Molecular architecture of a miRNA-regulated 3′ UTR. RNA *14*, 1297–1317.
39. Yamamoto, Y., Yagita, K., and Okamura, H. (2005). Role of cyclic mPer2 expression in the mammalian cellular clock. Mol. Cell. Biol. *25*, 1912–1921.
40. Chen, R., Schirmer, A., Lee, Y., Lee, H., Kumar, V., Yoo, S.H., Takahashi, J.S., and Lee, C. (2009). Rhythmic PER abundance defines a critical nodal point for negative feedback within the circadian clock mechanism. Mol. Cell *36*, 417–430.
41. Landskron, J., Chen, K.F., Wolf, E., and Stanewsky, R. (2009). A role for the PERIOD:PERIOD homodimer in the Drosophila circadian clock. PLoS Biol. *7*, e3.
42. Ruaud, A.F., and Bessereau, J.L. (2006). Activation of nicotinic receptors uncouples a developmental timer from the molting timer in C. elegans. Development *133*, 2211–2222.
43. Koh, K., and Rothman, J.H. (2001). ELT-5 and ELT-6 are required continuously to regulate epidermal seam cell differentiation and cell fusion in C. elegans. Development *128*, 2867–2880.
44. Simonetta, S.H., Migliori, M.L., Romanowski, A., and Golombek, D.A. (2009). Timing of locomotor activity circadian rhythms in Caenorhabditis elegans. PLoS ONE *4*, e7571.
45. Myers, E.M., Yu, J., and Sehgal, A. (2003). Circadian control of eclosion: interaction between a central and peripheral clock in Drosophila melanogaster. Curr. Biol. *13*, 526–533.
46. Kyriacou, C.P., Oldroyd, M., Wood, J., Sharp, M., and Hill, M. (1990). Clock mutations alter developmental timing in Drosophila. Heredity *64*, 395–401.
47. Tennessen, J.M., and Thummel, C.S. (2008). Developmental timing: let-7 function conserved through evolution. Curr. Biol. *18*, R707–R708.
48. Pasquinelli, A.E., Reinhart, B.J., Slack, F., Martindale, M.Q., Kuroda, M.I., Maller, B., Hayward, D.C., Ball, E.E., Degnan, B., Müller, P., et al. (2000). Conservation of the sequence and temporal expression of let-7 heterochronic regulatory RNA. Nature *408*, 86–89.
49. Hammell, C.M., Karp, X., and Ambros, V. (2009). A feedback circuit involving let-7-family miRNAs and DAF-12 integrates environmental signals and developmental timing in Caenorhabditis elegans. Proc. Natl. Acad. Sci. USA *106*, 18668–18673.
50. Bethke, A., Fielenbach, N., Wang, Z., Mangelsdorf, D.J., and Antebi, A. (2009). Nuclear hormone receptor regulation of microRNAs controls developmental progression. Science *324*, 95–98.
51. Van Wynsberghe, P.M., Kai, Z.S., Massirer, K.B., Burton, V.H., Yeo, G.W., and Pasquinelli, A.E. (2011). LIN-28 co-transcriptionally binds primary let-7 to regulate miRNA maturation in Caenorhabditis elegans. Nat Struct Mol Biol *18*, 302–308.
52. Szewczyk, N.J., Udranszky, I.A., Kozak, E., Sunga, J., Kim, S.K., Jacobson, L.A., and Conley, C.A. (2006). Delayed development and lifespan extension as features of metabolic lifestyle alteration in C. elegans under dietary restriction. J. Exp. Biol. *209*, 4129–4139.
53. Knight, C.G., Patel, M.N., Azevedo, R.B., and Leroi, A.M. (2002). A novel mode of ecdysozoan growth in Caenorhabditis elegans. Evol. Dev. *4*, 16–27.
54. Ruaud, A.F., Katic, I., and Bessereau, J.L. (2011). Insulin/Insulin-like growth factor signaling controls non-Dauer developmental speed in the nematode Caenorhabditis elegans. Genetics *187*, 337–343.
55. van der Linden, A.M., Beverly, M., Kadener, S., Rodriguez, J., Wasserman, S., Rosbash, M., and Sengupta, P. (2010). Genome-wide analysis of light- and temperature-entrained circadian transcripts in Caenorhabditis elegans. PLoS Biol. *8*, e1000503.
56. Epstein, H.F., and Shakes, D.C., eds. (1995)., Caenorhabditis elegans: Modern Biological Analysis of an Organism, *Volume 48* (San Diego: Academic Press).